Studies on the salt concentration of a PVdF–PVC based polymer blend electrolyte

S. Rajendran [a,*], P. Sivakumar [b], Ravi Shanker Babu [a]

[a] *Department of Physics, Alagappa University, Karaikudi 630003, India*
[b] *Department of Physics, H.H. The Rajah's College, Pudukkottai 622001, India*

Abstract

To investigate the effects of salt concentration, LiBF$_4$ was incorporated into a PVdF–PVC based polymer blend and thin electrolytes were prepared by solution casting technique. The obtained thin films were subjected to various characterizations such as FTIR, XRD and TG/DTA analysis to study their complex behaviour, amorphicity and thermal stability, respectively. The ionic conductivities of the electrolytes were measured by AC impedance. A PVdF (80)–PVC (20)–LiBF$_4$ (8 wt%) polymer electrolyte was found to have high conductivity compared to other complexes. Similar investigations were also repeated with a LiClO$_4$ salt in the above blend and the electrical conductivity was found to be higher in the polymer complex having 8 wt% of salt concentration.
© 2006 Published by Elsevier B.V.

Keywords: Polymer blend; FTIR; XRD; SEM; Thermal and conductivity studies

1. Introduction

Solid polymer electrolytes (SPE) are currently receiving a great deal of attention because of their proposed large scale use in secondary lithium ion batteries and electro-chromic smart windows [1,2]. In the recent past, most in-depth efforts have focused on the PEO, PAN, PVC, PMMA, PVdF and blend based SPEs to improve their electrical conductivity at ambient temperature [3–8]. Even though these materials exhibit favorable mechanical properties, their conductivities are not high at room temperature. In order to improve the conductivity, several approaches have been made to overcome this limitation without sacrificing mechanical integrity, including the use of a flexible, low glass transition temperature (T_g) polymer host [9] and by adding plasticizing agents to these polymers. Moreover, the addition of a salt has a highly disturbing effect on the arrangement of the polymer chains and the ensuing conductivity. In order to realize a high lithium ion conduction: (i) a polymer should have compatibility with inorganic salts and their disassociated ions, (ii) a

polymer should provide a connected polar domain as the conduction path and (iii) a polymer should not interact with carrier ions too strongly in order to avoid complete trapping of carrier ions.

In order to focus on the above parameters, an appropriate amount of salt is necessary to achieve a favorable conductivity in lithium ion battery electrolytes. In the present study, polymer films consisting of PVdF (80)–PVC (20) – with the different weight ratios of salts such as LiBF$_4$ and LiClO$_4$ were prepared to optimize the salt concentration and achieve the highest conductivity. Throughout this investigation, PVdF and PVC were kept constant as an 80:20 wt% (PVdF–PVC) as in our earlier work [10].

2. Experimental

PVdF with average molecular weights of 5.34×10^5 (Aldrich) and PVC with an average molecular weight of 1.5×10^5 (Aldrich) were used in this study. LiBF$_4$ (Aldrich) and LiClO$_4$ were used after drying in vacuum at $100\,^\circ$C for 10 h. As in earlier investigations [10], PVdF–PVC were kept constant at a ratio of 4:1 wt%. PVdF, PVC and appropriate quantities of LiBF$_4$ (i.e. 4, 6, 8, 10 and 12 wt%) were dissolved in distilled tetrahydrofuran (THF) (E-Merck, Germany) and the

polymer solution was stirred continuously until a homogeneous viscous liquid was formed. The resulting solution was poured onto a finely cleaned glass plate and the solvent was allowed to evaporate at room temperature. This procedure has provided mechanically stable and freestanding films with the thickness of about 50–100 μm. These electrolytes were further dried for 24 h in vacuum at 60 °C to remove any trace of THF. Similar investigations were also carried out with $LiClO_4$ as salt on PVdF–PVC polymer blends. Film preparation and conductivity measurements were performed inside a glove box.

The prepared electrolytes were subjected to FTIR, XRD, SEM and TG/DTA studies. ABB Bomem MB 104 IR Spectrometer was used for FTIR measurements. Bruker, D8 Advance X-ray diffractometer was used to analyze the structural behaviour of the polymer electrolytes. A Perkin-Elmer, Pyris Diamond thermal analyzer was used for thermal analysis. Thermal analysis was performed in a nitrogen atmosphere at a heating rate of 10 °C min^{-1}. AC impedance measurements were carried out in the frequency range 40 Hz–100 kHz using a LCZ meter (model 3330, Keithley Instruments) with a signal amplitude of 10 mV. The conductivity values were obtained from the bulk resistance, in the complex impedance diagram, for different temperatures (303–373 K).

3. Results and discussion

3.1. X-ray diffraction studies

XRD patterns of pure PVdF, PVC, $LiBF_4$, $LiClO_4$ and its complexes are shown in Figs. 1 and 2. Figs. 1 and 2 show more amorphous phase, which may be due to the addition of salts such as $LiBF_4$ and $LiClO_4$ to the PVdF–PVC polymer blend. Generally, all polymer complexes seem to be more crystalline compared with the host polymer. The addition of salt at various weight percent induces a significant disorder in the polymer structure, hence the crystallinity of polymers, as evident from the broad peak obtained at $2\theta = 20.5$ °C in Fig. 1d–h. Similar changes were also observed in the Fig. 2d–h with the addition of $LiClO_4$ as the salt in the polymer blend. Invariably salt, a less intense and broad peak has been observed at $2\theta = 20.32$ °C in all complexes. The broad XRD peak revealed that the polymer blend containing 8 wt% of salt is more amorphous. This leads to high ionic conductivity. Peaks for the pure salt have completely disappeared in the polymer complexes. This confirmed that the polymer electrolytes have completely absorbed the salt.

3.2. FTIR studies

FTIR spectra of pure PVdF, PVC, $LiBF_4$, $LiClO_4$, PVdF (80)–PVC (20)–$LiBF_4$ and PVdF (80)–PVC (20)–$LiClO_4$ complexes are shown in Figs. 3 and 4. FTIR spectra of PVdF–PVC–$LiBF_4$/$LiClO_4$ complexes for the range of 2000–400 cm^{-1} are depicted in Figs. 5 and 6. It is observed from the FTIR spectra that no peaks have occurred from 4000–3100 cm^{-1} corresponding to the OH groups, which confirms that the samples are free from moisture. The absorption peaks of pure PVdF (2980, 1716, 1407, 1224 and 857 cm^{-1}), PVC (2913, 1426, 690 and
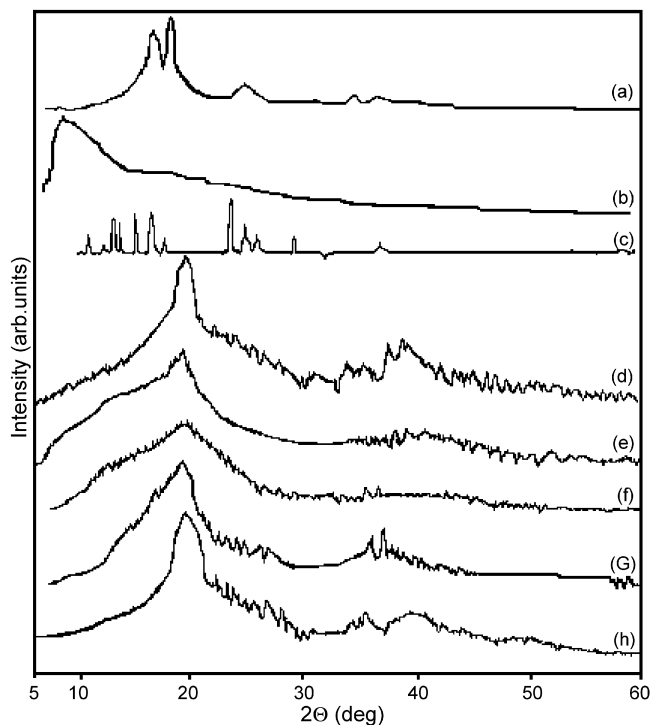

Fig. 1. XRD spectra of pure: (a) PVdF, (b) PVC, (c) $LiBF_4$, (d) PVdF (80)–PVC (20)–$LiBF_4$ (4), (e) PVdF (80)–PVC (20)–$LiBF_4$ (6), (f) PVdF (80)–PVC (20)–$LiBF_4$ (8), (g) PVdF (80)–PVC (20)–$LiBF_4$ (10) and (h) PVdF (80)–PVC (20)–$LiBF_4$ (12).
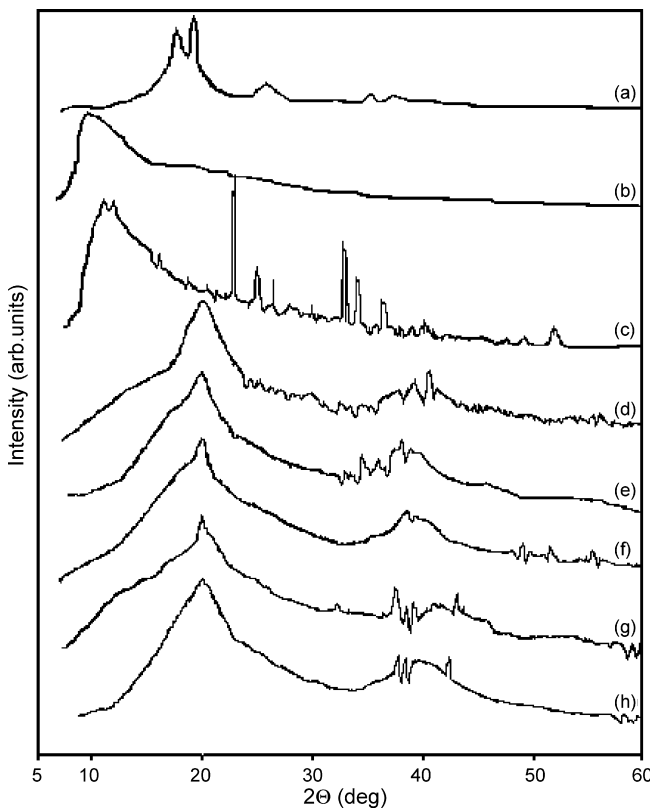

Fig. 2. XRD spectra of pure: (a) PVdF, (b) PVC, (c) $LiClO_4$, (d) PVdF (80)–PVC (20)–$LiClO_4$ (4), (e) PVdF (80)–PVC (20)–$LiClO_4$ (6), (f) PVdF (80)–PVC (20)–$LiClO_4$ (8), (g) PVdF (80)–PVC (20)–$LiClO_4$ (10) and (h) PVdF (80)–PVC (20)–$LiClO_4$ (12).
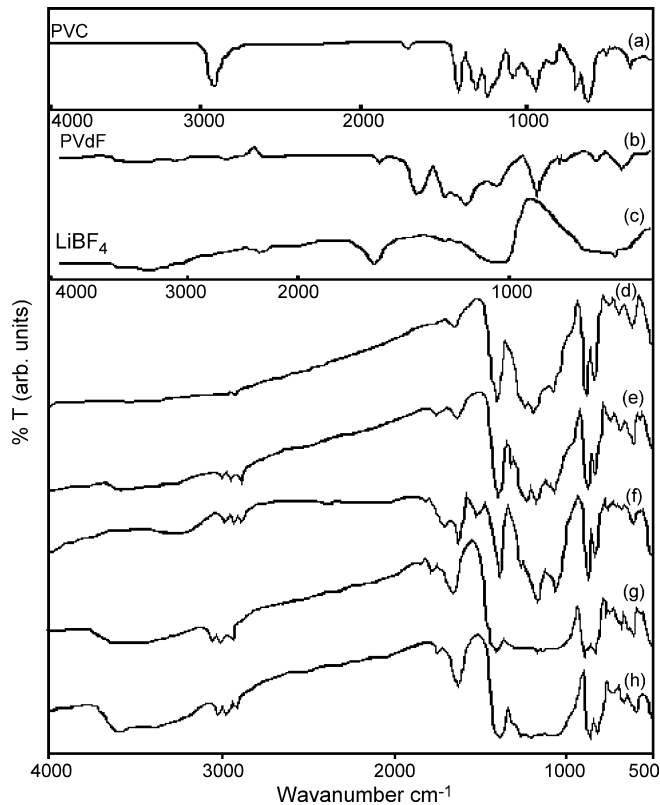
Fig. 3. FTIR spectra of pure: (a) PVC, (b) PVdF, (c) LiBF$_4$, (d) PVdF (80)–PVC (20)–LiBF$_4$ (4), (e) PVdF (80)–PVC (20)–LiBF$_4$ (6), (f) PVdF (80)–PVC (20)–LiBF$_4$ (8), (g) PVdF (80)–PVC (20)–LiBF$_4$ (10) and (h) PVdF (80)–PVC (20)–LiBF$_4$ (12).

Fig. 4. FTIR spectra of: (a) PVC, (b) PVdF, (c) LiClO$_4$, (d) PVdF (80)–PVC (20)–LiClO$_4$ (4), (e) PVdF (80)–PVC (20)–LiClO$_4$ (6), (f) PVdF (80)–PVC (20)–LiClO$_4$ (8), (g) PVdF (80)–PVC (20)–LiClO$_4$ (10) and (h) PVdF (80)–PVC (20)–LiClO$_4$ (12).

603 cm^{-1}) and LiBF$_4$ (1633 and 1320 cm^{-1}) have shifted to (2975, 1723, 1405, 1234 and 838 cm^{-1}), (2910, 1404, 682 and 611 cm^{-1}) and (1644 and 1321 cm^{-1}), respectively, in Fig. 3d–h. The absorption peak at 2957 cm^{-1} has shifted to 2973 cm^{-1} and the vibrational peaks at 1097 and 1463 cm^{-1} in LiClO$_4$ are disappeared in the Fig. 4d–h. The vibrational peaks in PVdF (796 and 532 cm^{-1}), PVC (1426, 1256 and 1096 cm^{-1}) and LiBF$_4$ (2346 cm^{-1}) are absent in the polymer complexes. The vibrational peaks 1328, 1234, 686 and 610 cm^{-1} are assigned to CH$_2$ deformation, in-plane CH deformation, C—Cl stretching and *cis*-CH wagging in PVC. The absorption peaks at 1655, 1404 and 1235 cm^{-1} are due to C=C stretching, C—F stretching and very strong mode of —CF$_2$— ring breathing vibrational modes in PVdF, which are clearly evident in Figs. 5 and 6. The absorption band appearing at 838 cm^{-1} may be assigned to the characteristic frequency of vinylidene compounds. The absorption band at 940 cm^{-1} is assigned to the formation of the perchlorate anion [11] and is shifted to 975 cm^{-1} in the polymer complexes. Further, this peak has again shifted to 985 cm^{-1}, which is evident in Fig. 5. This implies the aggregation of multiple ions when the salt concentration is increased (>8 wt%). Moreover the vibrational peak observed at 712 cm^{-1} is attributed to Li ions and it shifted to 740 cm^{-1} in polymer complexes with weak intensity and the characteristics frequencies related to the BF$_4^-$ and ClO$_4^-$ ions had no obvious changes, hence it was assumed that the interaction inside the system mainly occurred between the
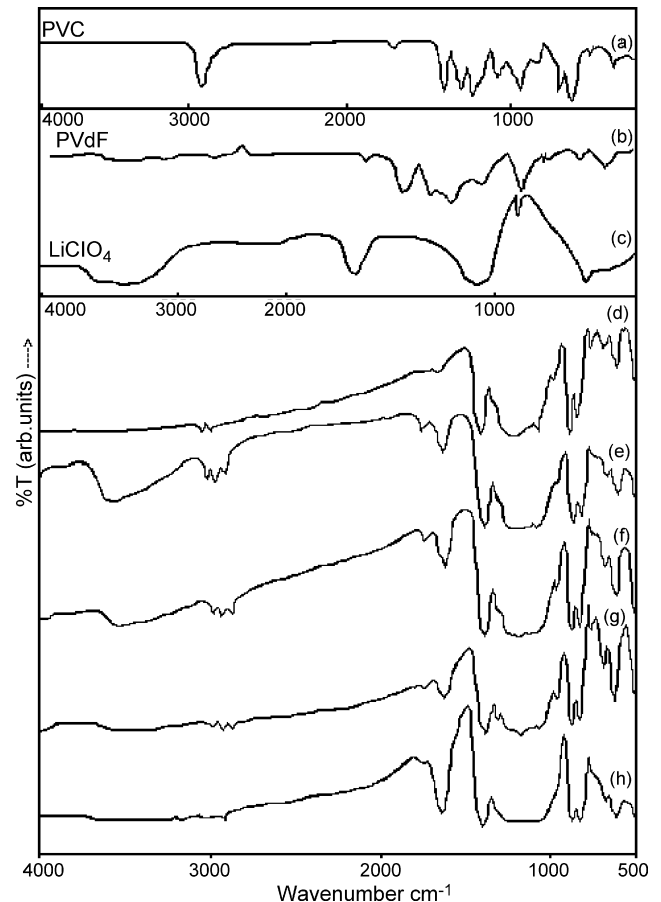
Li ions and the polymer chain molecules. As the salt content in the complex increases, the peak intensities of the bands first decrease up to 8 wt%, which corresponds to maximum conductivity. With further increases of salt concentration (i.e. >8%), the peak intensity of the electrolytes also increases. Consequent to this, a decrease in conductivity is observed. This is an indication that the complex becomes more ordered when the salt content increases beyond a particular concentration (i.e. 8 wt%) of LiBF$_4$ and LiClO$_4$.

3.3. Thermal analysis

The Thermogravimetric and differential thermal analyses for PVdF (80)–PVC (20)–LiBF$_4$ (8 wt%) and PVdF (80)–PVC (20)–LiClO$_4$ (8 wt%) are depicted in Fig. 7. The TG curve shows a gradual weight loss of about 10–12% from room temperature to 95 °C, which is due the evaporation of moisture in the polymer electrolyte or may be due to the evaporation of fluorine [12,13]. Volatilization of monomers and oligomers adsorbed in the matrix can also be responsible for this initial weight loss [14]. The second weight loss of about 20% occurred at around 296 °C as shown in Fig. 6a and b, may be due to the decomposition of the polymer electrolyte. From the DTA curve, it is
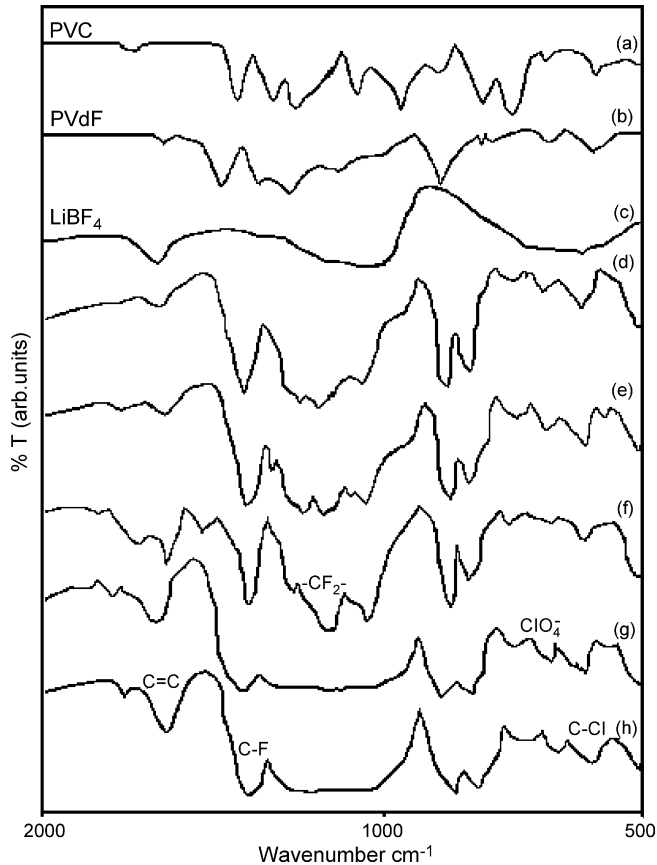
Fig. 5. FTIR spectra of the range of 2000–400 cm^{-1} for PVC, PVdF, LiBF$_4$ and PVdF (80)–PVC (20)–LiBF$_4$ (x%) (where x = 4, 6, 8, 10, 12).
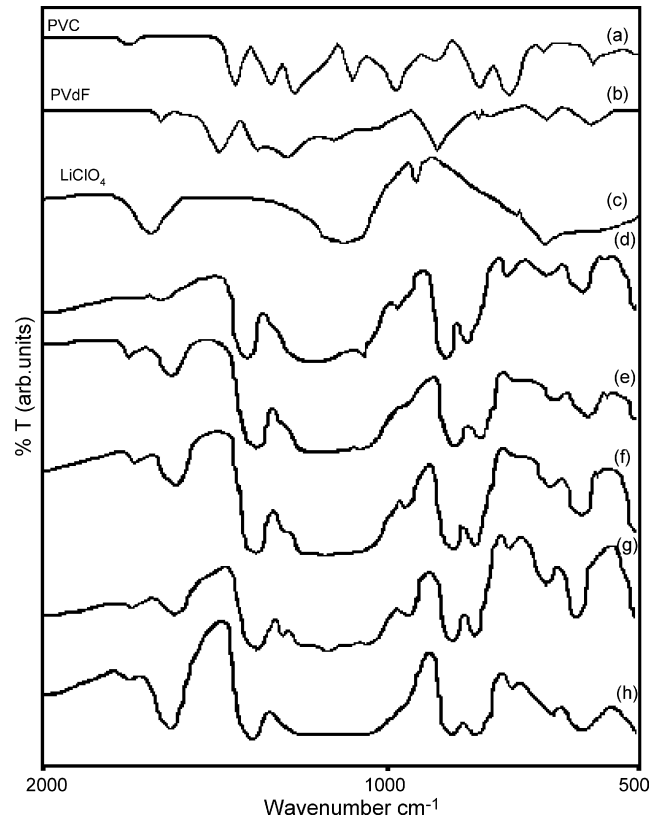

Fig. 6. FTIR spectra of the range of 2000–400 cm^{-1} for PVC, PVdF, LiClO$_4$ and PVdF (80)–PVC (20)–LiClO$_4$ (x%) (where x = 4, 6, 8, 10, 12).

observed that the endothermic peak at 162 °C reveals the melting temperature of PVDF, which is in good agreement with the value reported by Muniyandi et al. [15] and Jiang et al. [16] in DSC discussion on PVdF based gel electrolytes. The gradual weight loss of about 3–5% at 100–200 °C is attributed to the decomposition of low molecular weight compounds in the complex. The second weight loss with increased temperature is a consequence of the increase in T_g value [17]. The endothermic peak occurred at about 300 °C, reveals the complete decomposition of polymer electrolytes with the weight loss of about 30% in the complexes. This result indicates that the electrolyte is stable over 200 °C and is preferred in the lithium polymer batteries.

3.4. Electrical conductivity studies

The room temperature conductivity of the polymer electrolytes with different salt ratios has been measured by complex impedance spectroscopy. Fig. 8 illustrates the impedance pattern of PVdF (80)–PVC (20)–LiBF$_4$ and PVdF (80)–PVC (20)–LiClO$_4$ systems containing 8 wt% of salt in polymer blend at room temperature. Fig. 7 shows an arc followed by a slanted spike, which represents the high frequency semi circular region can be attributed to the electrolyte resistance. The intercept of the curve on the real axis gives the bulk resistance of the electrolyte (R_b). The electrical conductivity of the electrolyte
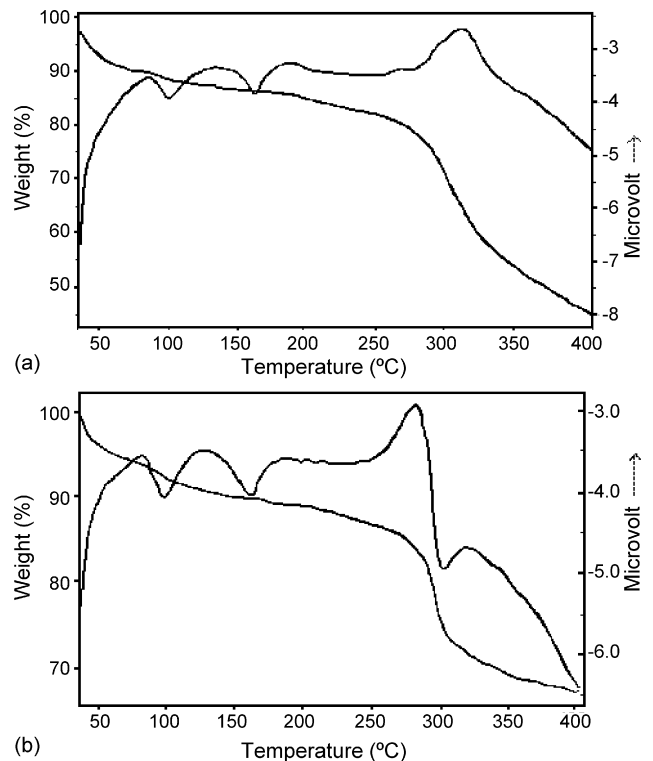

Fig. 7. TG/DTA plots for: (a) PVdF (80)–PVC (20)–8% of LiBF$_4$ and (b) PVdF (80)–PVC (20)–8% of LiClO$_4$.
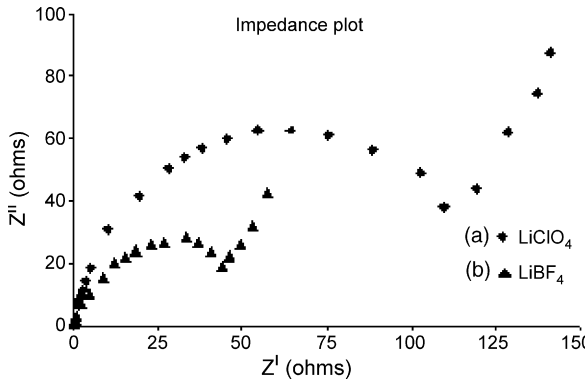
Fig. 8. Impedance diagram of: (a) PVdF (80)–PVC (20)–8% of LiBF$_4$ and (b) PVdF (80)–PVC (20)–8% of LiClO$_4$ at 304 K.
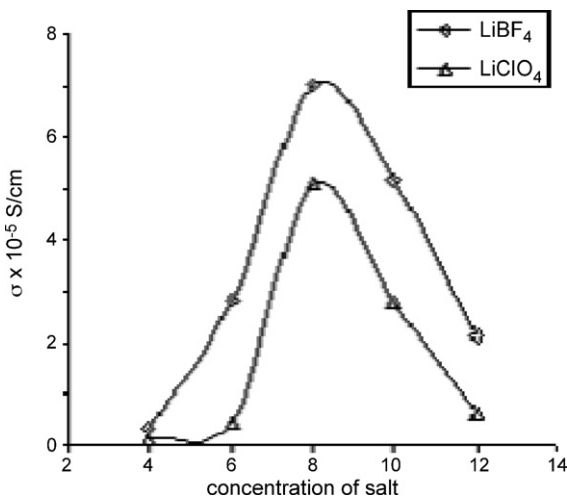

Fig. 9. Concentration of salt vs. room temperature conductivity.

Fig. 10. Arrhenius plots of log (σ) against reciprocal temperature for: (a) PVdF (80)–PVC (20)–x% of LiBF$_4$ and (b) PVdF (80)–PVC (20)–x% of LiClO$_4$, (where $x = 4$, 6, 8, 10 and 12 wt%).

was measured from the observed bulk resistance for the known thickness and surface area of the film. It is observed that the conductivity values of PVdF–PVC–Li salt complexes are 10^3 times higher than the host polymer. The highest room temperature conductivities observed at the salt concentration of 8 wt% for PVdF (80)–PVC (20)–LiBF$_4$/LiClO$_4$ (8 wt%) complexes
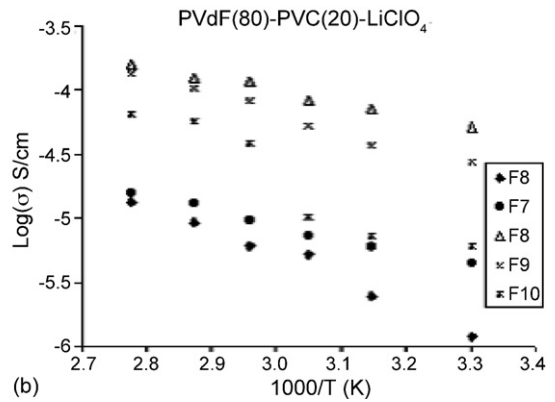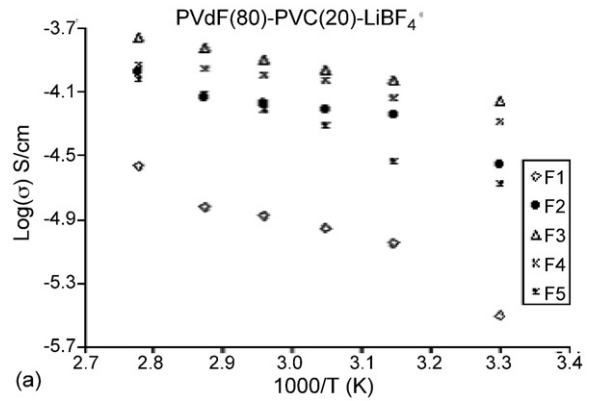
are 7.026×10^{-5} and 5.781×10^{-5} S cm^{-1}, respectively. The improved ionic conductivity is due to the enhancement of the ionic mobility and the larger number of carrier ions as already reported [18]. The conductivity of the polymer electrolyte initially increases due to the increment of the number of charge carriers being introduced into the complex, which is evident from Table 1. As the salt concentration increases, the number of carrier ions and T_g of the complex increase and this leads to stronger ion–ion interactions and, thereby, possibly impedes the

Table 1
Conductivity values of (10^{-5} S cm^{-1}) PVdF–PVC–x% of salt

Complex	Temperature					
	303 K	318 K	328 K	338 K	348 K	360 K
PVdF (80)–PVC (20)–LiBF$_4$ (x%)						
$x = 4$%	3.14E−06	8.97E−06	1.11E−05	1.34E−05	1.51E−05	2.73E−05
$x = 6$%	2.81E−05	5.66E−05	6.17E−05	6.72E−05	7.37E−05	1.07E−04
$x = 8$%	7.03E−05	9.32E−05	1.08E−04	1.25E−04	1.49E−04	1.73E−04
$x = 10$%	5.18E−05	7.32E−05	9.47E−05	1.03E−04	1.10E−04	1.17E−04
$x = 12$%	2.11E−05	2.92E−05	4.87E−05	6.24E−05	7.76E−05	9.66E−05
PVdF (80)–PVC (20)–LiClO$_4$ (x%)						
$x = 4$%	1.21E−06	2.48E−06	5.31E−06	6.17E−06	9.28E−06	1.35E−05
$x = 6$%	4.46E−06	5.93E−06	7.38E−06	9.51E−06	1.29E−05	1.58E−05
$x = 8$%	5.10E−05	7.26E−05	8.26E−05	1.15E−04	1.25E−04	1.55E−04
$x = 10$%	2.79E−05	3.71E−05	5.32E−05	8.25E−05	1.04E−04	1.34E−04
$x = 12$%	6.20E−06	7.37E−06	1.03E−05	3.83E−05	5.74E−05	6.48E−05

polymer backbone's segmental motion which ultimately causes a lowering of the conductivity [18], in other words, the higher concentration in the amorphous region may increase both the number of carrier ions and T_g. The decrease in ionic mobility due to the increasing of T_g seems to nullify the increase in the number of carrier ions at higher salt concentrations. Thus, the ionic conductivity decreases as the salt concentration increases, which is represented in the Fig. 9. A similar phenomenon occurs in PAN, PEO or PPO based electrolytes with the addition of LiClO$_4$ [19,20].

The temperature dependence of the electrical conductivity of PVdF–PVC containing various amounts of salt concentration such as LiBF$_4$ and LiClO$_4$ are shown in Fig. 10a and b. The conductivity of the electrolyte increases with increases of temperature. This implies that the increases conductivity does not originate from the SPEs residual organic solvent, but is purely due to the segmental motion of polymer backbone. As the temperature approaches the T_g of SPE, the polymer backbone's segmental motion is severe [21]. Thus, the present finding corroborates previous ones [22,23]. The temperature dependent conductivity plots follow Arrhenius behaviour of the electrolytes.
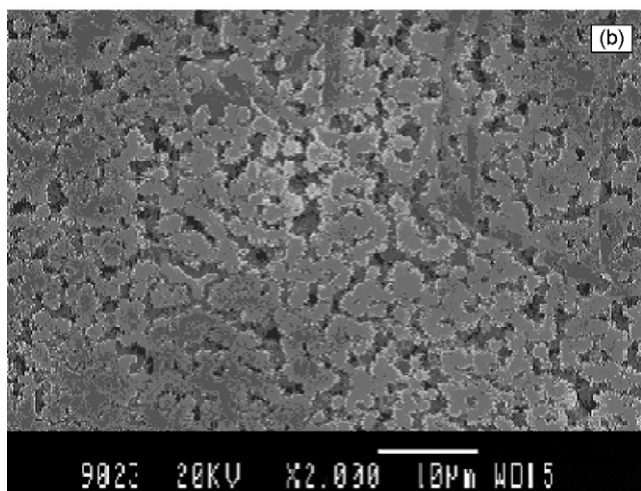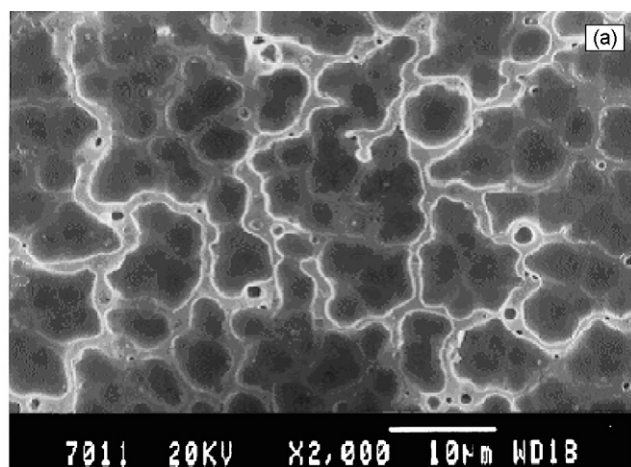

Fig. 11. SEM micrographs of: (a) PVdF (80)–PVC (20)–8% of LiBF$_4$ and (b) PVdF (80)–PVC (20)–8% of LiClO$_4$.

3.5. SEM studies

SEM photographs of PVdF (80)–PVC (20)–LiBF$_4$ (8 wt%) and PVdF (80)–PVC (20)–LiClO$_4$ (8 wt%) are shown in Fig. 11a and b, respectively. This indicates that there is no spherulitic structure due to the crystalline phase. The surfaces of the electrolytes show fine pores in the polymer matrix, which aid ion mobility. It is well known that the formation of the porous structure is a complex process that depends on the interaction of the solvent with the polymers and is kinetically controlled by the relative rates of evaporation of compounds. Furthermore, the size of the dispersed phase in Fig. 11a is larger than that in Fig. 11b. Due to the higher depressive phase, LiBF$_4$ complex were observed to have higher conductivity than LiClO$_4$ complex.

4. Conclusion

Polymer electrolytes based on PVdF–PVC with LiBF$_4$/LiClO$_4$ as the salt at different concentrations were prepared using a solvent casting technique. The highest room temperature ionic conductivity was observed for a salt concentration of 8 wt% for both LiBF$_4$ and LiClO$_4$ based polymer complexes. The conductivity results for all polymer electrolytes showed very similar Arrhenius type behaviour, irrespective of the salt concentrations. The XRD studies explained the occurrence of complexation in amorphous phase and TG/DTA revealed the thermal stability of the electrolytes. The FTIR studies confirmed the strong coordination between the molecules of PVdF–PVC and lithium salt. The maximum room temperature conductivity value was found in PVdF (80)–PVC (20)–LiBF$_4$ (8 wt%) and PVdF (80)–PVC (20)–LiClO$_4$ (8 wt%) systems.

References

[1] F.M. Gray, Solid Polymer Electrolytes, VCH publishers Inc., New York, 1991.
[2] J.R. MacCallum, C.A. Vincent (Eds.), Polymer Electrolytes Reviews, vol. 2, Elsevier Applied Science, London, 1989.
[3] K.M. Abraham, M. Alamgir, J. Electrochem. Soc 137 (1990) 1657.
[4] M. Watanable, M. Kanba, K. Nagaoka, I. Shinohara, Polym. Sci. Polym. Phys. Ed. 21 (1983) 939.
[5] M. Alamgir, K.M. Abragam, J. Electrochem. Soc. 140 (1993) L96.
[6] O. Bohnke, G. Frand, M. Rezrazi, C. Rousslot, C. Truche, Solid State Ionics 66 (1993) 97.
[7] E. Tsuchida, H. Ohno, K. Tsunemi, Electrochim. Acta 28 (1983) 591.
[8] S. Rajendran, O. Mahendran, T. Mahalingam, Eur. Polym. J. 38 (2002) 49.
[9] P.M. Blonsky, D.F. Shriver, P. Austin, H.R. Allcock, Solid State Ionics 18 (1986) 258.
[10] S.Rajendran, P.Sivakumar, R. S. Babu, Solid State Ionics, Communicated.
[11] D. Ostrovshii, A. Brodin, M. Torell, G.B. Appetecchi, B. Scrosati, J. Chem. Phys. 109 (1998) 7618.
[12] T. Shodai, B.B. Owens, Oh. Suke, J. Yamakai, J. Electrochem. Soc. 141 (1994) 2978.
[13] D.R. Payne, P.V. Wright, Polymer 23 (1982) 690.
[14] V. Mano, M.I. Felisbersti, T. Matencio, M.A. De Paoli, Polymer 37 (1996) 5165.
[15] N. Muniyandi, N. Kalaiselvi, P. Periyasamy, R. Thirunakaran, B.R. Babu, S. Gopukumar, T. Premkumar, N.G. Renganathan, M. Ragavan, J. Power Sources 96 (2001) 14.
[16] Z. Jiang, B. Corroll, K.M. Abraham, Electrochim. Acta 42 (17) (1997) 2667.

[17] S. Ramesh, A.K. Arof, J. Power Sources 90 (2001) 41.

[18] J.M.G. Cowie, in: J.R. MacCallum, C.A. Vincent (Eds.), Polymer Electrolytes Reviews, vol. 1, Elsvier, Applied Science, London, 1987, p. 92.

[19] B. Huang, et al., Solid State Ionics 85 (1996) 79.

[20] M. Watanable, S. Nagano, N. Ogata, K. Sanui, Solid State Ionics 18–19 (1986) 338.

[21] C.R. Yang, J.T. Perng, Y.Y. Wang, C.C. Wan, J. Power sources 62 (1996) 89.

[22] K. Tsunemi, H. Ohno, E. Tsuchida, Electrochim. Acta 28 (1983) 833.

[23] B.L. Papke, M.A. Ratner, D.F. Shriver, J. Electrochem. Soc. 129 (1982) 1434.